Molecular Therapy
Nucleic Acids
Original Article

Characterization of a Prostate- and Prostate Cancer-Specific Circular RNA Encoded by the Androgen Receptor Gene

Jindan Luo,[1] Yinan Li,[2,3] Wei Zheng,[4] Ning Xie,[2] Yao Shi,[2] Zhi Long,[5] Liping Xie,[1] Ladan Fazli,[2] Dahong Zhang,[5] Martin Gleave,[2] and Xuesen Dong[2]

[1]Department of Urology, First Affiliated Hospital, School of Medicine, Zhejiang University, Hangzhou 310003, China; [2]Department of Urologic Sciences, University of British Columbia, Vancouver, BC, Canada; [3]Department of Vascular Surgery, Renji Hospital, School of Medicine, Shanghai Jiaotong University, Shanghai, China; [4]Department of Urology, Zhejiang Provincial People's Hospital, Hangzhou 310024, China; [5]Department of Urology, Third Xiangya Hospital, Central South University, Changsha 410013, China

The linear mRNAs transcribed under alternative RNA splicing and overexpression/amplification of the androgen receptor (*AR*) gene are poor prognostic biomarkers of castrate-resistant prostate cancer (PCa). Whether the *AR* gene also transcribes non-coding circular RNAs that are associated with PCa development and tumor progression remains unclear. Here, we identified and characterized an *AR* circular RNA, called circAR3, that is widely expressed in PCa cell models and prostate tumors. circAR3 can be secreted into culture media of PCa cell lines and is detectable in the serum from mice bearing PCa xenografts. In PCa patient tissues, circAR3 is highly expressed in benign prostate and hormone naive PCa but downregulated when tumors were treated with neoadjuvant hormone therapy and further reduced when tumors progressed to the castrate-resistant stage. However, circAR3 levels in plasma are extremely low in patients with benign prostate, are upregulated in PCa patients with high Gleason scores and lymph node metastasis, and become undetectable in men after radical prostatectomy. circAR3 does not affect AR signaling, PCa cell proliferation, and invasion rates. Our results demonstrated that the origin of the detectable plasma circAR3 is from the prostate/PCa. Plasma circAR3 may be developed to be a PCa biomarker to monitor PCa development and tumor progression.

INTRODUCTION

The mRNAs transcribed by the androgen receptor (*AR*) gene are markers of castrate-resistant prostate cancer (PCa) since they can reflect aberrant RNA splicing and overexpression and amplification of the *AR* gene. *AR* is the primary therapeutic target of metastatic PCa.[1,2] However, these tumors inevitably evade AR inhibition and progress to the lethal castrate-resistant prostate cancers (CRPCs)[3,4] through mechanisms including aberrant *AR* gene splicing to generate constitutively active splice variants,[5–9] *AR* gene overexpression and amplification,[10–12] and *AR* gain-of-function promiscuous mutations in the ligand-binding domain.[13–15] These findings rationalize that AR mRNAs from tumor biopsies, circulating tumor cells (CTCs), and patient plasma may serve as biomarkers to monitor PCa progression and therapy effectiveness.[16–21] An ideal AR mRNA biomarker would be (1) stable, resistant to RNase digestion, and easy to be collected; (2) expressed at relatively high levels to allow detection; and (3) carrying *AR* gene mutations to monitor CRPC progression. A clinical-grade assay detecting the mRNA of the AR-v7 splice variant in CTCs is provided by a clinical laboratory improvement amendments-certified lab at Johns Hopkins University.[22] Patients who receive AR pathway inhibitors (e.g., enzalutamide) are more likely resistant to these treatments if they are AR-v7 positive[8] but still remain sensitive to taxane chemotherapy. However, a major limitation preventing mRNAs from becoming widely used biomarkers in clinic is that they are linear forms of RNA and sensitive to RNA exonuclease digestion. And RNA exonucleases are abundantly present in patient tumors, plasma, and urine.

The discovery of non-coding RNA has widened our understanding of gene functions. Many non-coding RNAs have been demonstrated not only to be associated with human diseases with potentials to be developed into biomarkers, but also to exert biological functions shown by *in vitro* cell assays and *in vivo* genetically engineered mouse model studies.[23,24] Whole-transcriptome sequencing has revealed a class of non-coding RNAs, called circular RNAs (circRNAs), that is abundantly expressed accounting up to 10% of total RNAs in human cells.[25,26] Two recent studies reported widespread expression of circRNAs in prostate tumors.[27,28] In contrast to mRNAs, circRNAs are covalently closed circRNA molecules containing exon and/or intron sequences. Mutations at the splice sites flanking the circularized exons abolished circRNA formation, indicating that circRNAs

Received 28 May 2019; accepted 15 October 2019;
https://doi.org/10.1016/j.omtn.2019.10.015.

Correspondence: Xuesen Dong, Department of Urologic Sciences, University of British Columbia, 2660 Oak Street, Vancouver, BC V6H 3Z6, Canada.
E-mail: xdong@prostatecenter.com
Correspondence: Yinan Li, Department of Urologic Sciences, University of British Columbia, 2660 Oak Street, Vancouver, BC V6H 3Z6, Canada.
E-mail: liyinan0402@126.com

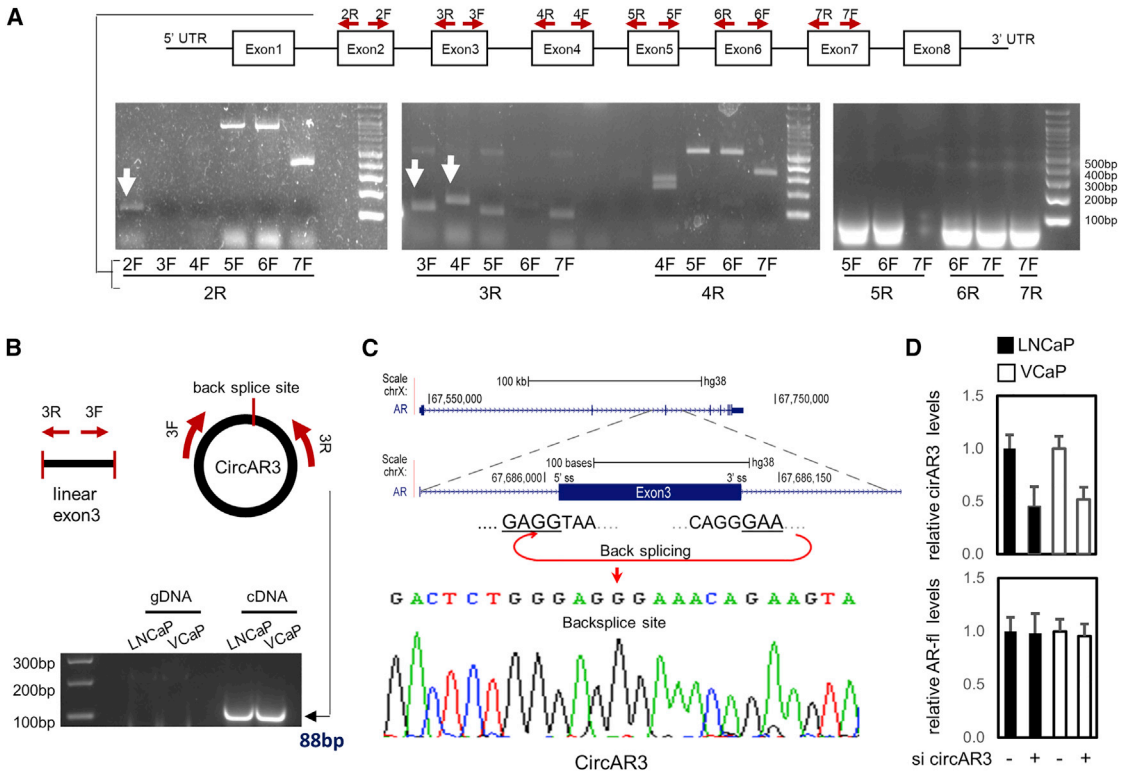

Figure 1. Validation of circAR3 Expression in PCa Cells

(A) Outward primers were designed to cover AR exons 2–7 and used to perform RT-PCR using each combination of primers as indicated and cDNA from VCaP cells. RT-PCR products were sub-cloned into pCR2.1 topo vector and subjected for Sanger sequencing. Arrows indicate that Sanger sequencing results confirmed the RT-PCR products containing the back-splice sites and flanking exon sequences from the AR gene. (B) Genomic DNA and cDNA from both LNCaP and VCaP cells were used as templates for RT-PCR with 3F and 3R primers. Amplicons were separated by DNA electrophoresis. (C) A diagram presents the human AR gene in chromosome X (RefSeq: NM_000044) and shows back splicing of exon 3 for circAR3. Sanger sequencing confirmed the back-splice site within the RT-PCR product shown in (B). (D) LNCaP and VCaP cells were transfected with control or siRNA targeting the back-splicing site of circAR3. Total RNA was isolated. circAR3 and AR-fl mRNA levels were measured by relative quantification of quantitative real-time PCR with GAPDH as the housekeeping gene.

are synthesized by the same machinery of RNA spliceosome for mRNAs.[29] circRNAs lack a polyadenylated tail and are less susceptible to degradation by RNA exonucleases. Their half-life in mammalian cells is 2.5 times longer than that of their linear counterparts.[30] circRNAs carry genetic information such as somatic mutations gained during anti-cancer therapy. Furthermore, certain circRNAs are enriched in exosomes that can be secreted into the bloodstream from its original organs. The longer half-life of circRNAs also contributes to the 6.3-fold higher levels of circRNAs in exosomes than in cells.[31] When profiling tumor phenotypes and designing suitable therapies, high stability and enrichment in exosome are important features for circRNAs to be potential biomarkers in liquid biopsy, because tissue biopsies in patients with metastatic tumors are not commonly performed. Identifying tumor-specific circRNAs from patient plasma may, therefore, lead to the development of diagnostic or prognostic biomarkers of tumors.

Whether the *AR* gene encodes circRNA in PCa cells and whether AR circRNA is detectable in patient plasma to diagnose PCa or monitor tumor progression remain undefined. Our understanding of the *AR* gene had been focused on the biology of AR proteins translated from linear mRNAs. Whether non-coding circRNAs of the *AR* gene have any biological functions warrants further investigation. We set out to determine whether AR circRNA is expressed in PCa cells, explore their potential to be a biomarker, and define possible roles in PCa cell biology.

RESULTS

Identification of circRNAs Encoded by the AR Gene in PCa Cells

To explore whether the *AR* gene encodes any circRNA, we designed a series of outward primers from exons 2–7 (Figure 1A), because these exons have both 5′ and 3′ canonical splice sites that can be recognized by RNA spliceosome for back splicing. We aimed at finding AR circRNAs that carry exon sequences useful for detecting *AR* somatic mutations during AR pathway inhibition therapy. AR circRNAs with intron sequences were not focused on in this study. We found three AR circRNAs that contain exons 2, 3, or 3 plus 4, respectively, in VCaP cells. All other amplicons were confirmed not from the *AR* gene by Sanger sequencing. Since the circRNA containing only exon 3 (designated as circAR3) is expressed 10- to 20-fold higher

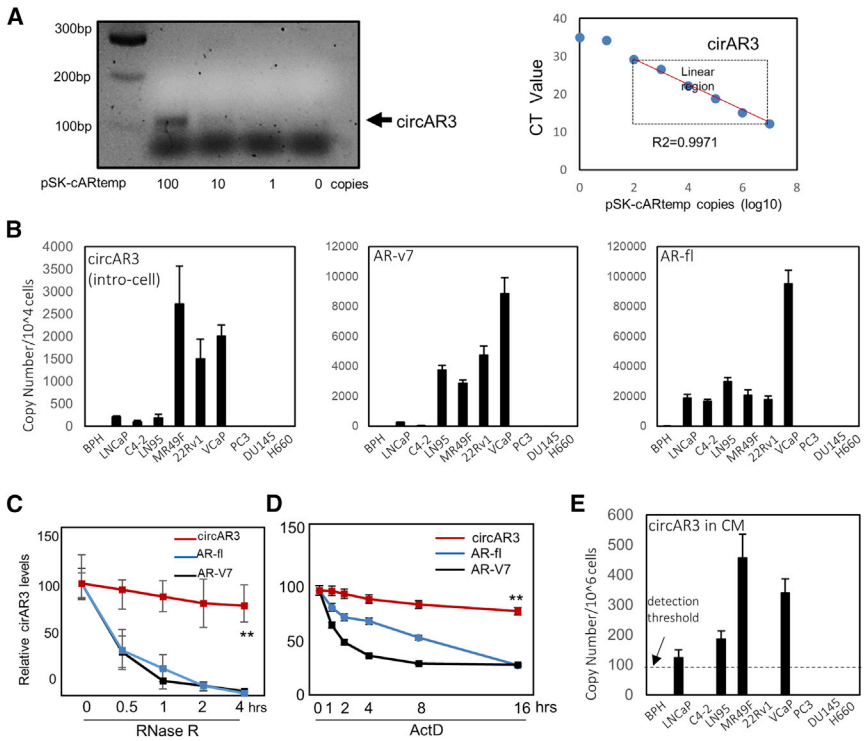

Figure 2. Quantification of circAR3 Levels by Quantitative Real-Time PCR

(A) A serial 10-fold dilution of pSK-cARtemp was used as templates to perform RT-PCR. Amplicons were separated by DNA electrophoresis. The diluted pSK-cARtemp was also used to perform quantitative real-time PCR to establish the standard curve of CT values over pSK-cARtemp copy numbers. The equation and R^2 value were calculated and used to calculate circAR3 copy numbers. The linear range of the standard curve was highlighted. (B) Total RNA was extracted from 1×10^4 cells from 10 prostate/PCa cell lines. circAR3, AR-fl, and AR-v7 copy numbers were determined by quantitative real-time PCR using absolute quantification. (C) Total RNA was extracted from the 22Rv1 cells and treated with RNase R with the ratio of 1 U RNase R/μg RNA for 0–4 h. Relative circAR3, AR-fl, and AR-v7 levels were determined by quantitative real-time PCR. (D) 22Rv1 cells were treated with 5 μM actinomycin D (ActD) RNA samples for 0–16 h. Relative circAR3, AR-fl, and AR-v7 levels were determined by quantitative real-time PCR. (E) Conditioned media from 1×10^6 prostate/PCa cells were collected. Cell-free RNA was extracted to measure circAR3 copy numbers by quantitative real-time PCR. All quantitative real-time PCR assays were repeated in three independent experiments that were performed in triplicate. One-way ANOVA followed by Tukey's test was used in pairwise comparison among different groups. Data were presented as the mean ± SD. **$p < 0.01$ when compared with controls.

than the other two AR circRNAs as confirmed by quantitative real-time PCR and circAR3 was also reported in the recent two publications[27,28] where RNA-sequencing (RNA-seq) technique was applied to globally profiled circRNAs in PCa tissues, our following studies focused on validating and characterizing circAR3 in PCa.

We applied three methods to validate circAR3 expression in PCa cells: (1) a pair of outward primers were used to perform RT-PCR (Figures 1A and 1B). These primers should not result in amplicons derived from linear *AR* mRNA in the predicted sizes. Total RNA from LNCaP and VCaP cells was subjected to reverse transcription followed by PCR. An amplicon with a correct predicted size of 88 bp was detected by DNA agarose gel electrophoresis (Figure 1B). (2) This 88-bp amplicon was also subjected to Sanger sequencing that confirmed the back-splice site and its flanking sequences were from AR exon 3 in a closed-loop structure (Figure 1C). (3) RNA silencing was performed to target the back-splicing site of circAR3 in both LNCaP and VCaP cells, resulting in significant reduction of circAR3 but not full-length AR (AR-fl) mRNA levels (Figure 1D). Together, these results confirmed that circAR3 is expressed in VCaP and LNCaP cells.

Quantification of circAR3 Levels by Quantitative Real-Time PCR

Accurate measurement of the number of circRNAs is challenging because the routinely used relative quantification method of quantitative real-time PCR relies on the presence of mRNAs of housekeeping genes, which will be difficult when mRNA detection is not possible (e.g., mRNAs are rapidly degraded in patient plasma or urine). We chose the absolute quantification method for circAR3 measurement. However, a threshold of cycle threshold (CT) value is needed to determine the true positivity of an amplicon of circAR3. To achieve this, we first cloned the RT-PCR product from Figure 1B into the pSK vector to generate pSK-cARtemp. Copy numbers of pSK-cARtemp were calculated as follows: copy number (molecules/μL) = concentration (g/μL)/(bp size of double-stranded product × 660) × 6.022×10^{23}. A serial of 10-fold dilution of the pSK-cARtemp vector was used as a template for RT-PCR. When the PCR products were separated by DNA gel electrophoresis, a solid DNA band was visualized when 100 copies of pSK-cARtemp were used (Figure 2A). Next, a serial dilution of the pSK-cARtemp vector was used as templates to perform quantitative real-time PCR. A standard curve was generated by the $\log_{10}$ copy numbers of pSK-cARtemp versus corresponding CT values. The linear regression of CT values (12.1–29.1) fell in between 10^2 and 10^7 copies of the template. CT values obtained from 0 and 10 copies of the template were similar. These results indicated that the detection threshold is ~100 copies of the template with CT value at ~29.1 in quantitative real-time PCR assays. Samples that have < 100 copies of circAR3 or give a CT value > 29.1 means that the real-time PCR signal is not reliable. These samples were deemed circAR3 negative in the following study.

circAR3 Expression in *In Vitro* PCa Cell Models

We showed that all AR-positive (e.g., LNCaP, LNCaP95, C4-2, 22Rv1, VCaP, and MR49F), but not AR-negative (e.g., PC3, DU145, and NCI-H660) PCa cell lines express circAR3. The results indicated that the

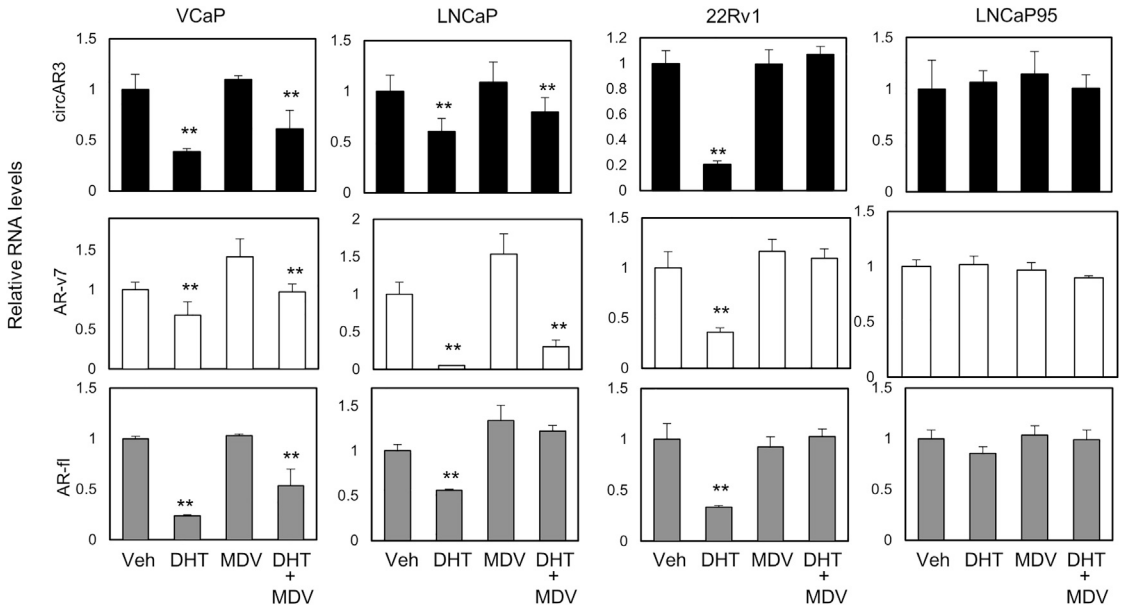

Figure 3. AR Signaling Regulates circAR3 Expression

VCaP, LNCaP, 22Rv1, and LN95 cells were cultured in media containing 5% CSS for 48 h. Cells were treated with vehicle, 10 nM DHT, and/or 5 μM MDV3100 for 24 h. Relative RNA levels of circAR3, AR-fl, and AR-v7 were determined by quantitative real-time PCR and normalized to the GAPDH housekeeping gene. All assays were repeated in three independent experiments that were performed in triplicate. One-way ANOVA followed by Tukey's test was used in pairwise comparison among different groups. Data were presented as the mean ± SD. **$p < 0.01$ when compared with controls.

expression of circAR3 relies on AR gene transcription. LNCaP cells have ~200 copies/μg total RNA of circAR3 (Figure 2B). VCaP and 22Rv1 cells bearing AR gene amplification or AR gene/exon3 rearrangement have 2,000 and 1,500 copies/μg of total RNA of circAR3, respectively. MR49F cells, which are LNCaP-derived enzalutamide-resistant PCa cells,[32] contain 2,700 copies/μg of total RNA of circAR3. We found that the ratio of circAR3 to AR-v7 ranges from 0.05 in LNCaP95 cells to 1.8 in C4-2 cells. These results indicated that although the positivity of circAR3 expression is correlated with AR-v7 expression, the absolute levels of circAR3 and AR-v7 are not necessarily proportional to each other. This is likely explained by the different rates of RNA splicing of circAR3 and AR-v7, even though they are processed from the same AR pre-mRNA by RNA splicing machinery.

Although less circAR3 was synthesized than AR-v7 and AR-fl mRNAs in cells, circAR3 showed higher stability in the presence of RNase R or actinomycin D (ActD) treatment (Figures 2C and 2D). Furthermore, circAR3 but not AR-v7 and AR-fl was detectable in the conditioned media of several AR-positive PCa cell models (Figure 2E). These results may be explained by that circAR3 but not AR mRNAs is secreted into culture media possibly in exosomes, or by that circAR3 has higher stability than AR mRNAs to resist RNA exonuclease digestion.

circAR3 Expression Is Regulated by AR Inhibition in PCa Cell Models

The transcription of AR-v7 is upregulated by AR inhibition due to increased *AR* transcription rate. To study whether AR inhibition regulates circAR3 biosynthesis, we treated LNCaP, VCaP, 22Rv1, and LNCaP95 cells with either vehicle, Dihydrotestosterone (DHT), and/or enzalutamide (Figure 3). circAR3 levels were suppressed by DHT comparing androgen deletion or enzalutamide treatment conditions in LNCaP, VCaP, and 22Rv1 cells, but not in androgen-insensitive LNCaP95 cells. Although changes in circAR3 levels followed the similar trends of AR-fl and AR-v7 mRNAs, these changes were not proportional to each other. These findings suggest that circAR3 biosynthesis is regulated by AR signaling in a cell-context-dependent manner.

Detection of circAR3 in PCa Patient Tumor Samples

To determine circAR3 expression in prostate tumors from patients, we applied RNA *in situ* hybridization (RISH) techniques with a Basecope probe (ACDBio, USA) against the back-splice site of circAR3. The specificity of this probe was validated by using VCaP cells that serve as a circAR3 positive control. Additional control experiments included a negative control probe against the *dapB* gene from bacteria that should not recognize any human gene products, and a positive control probe against human *PPIB* gene (Figure 4A). When the circAR3 probe was used to hybridize tissue microarrays (TMAs) containing benign prostate and primary PCa with various Gleason scores, we found that RISH signals were detected in both prostate epithelium and stroma (Figure 4B). There were no differences in circAR3 expression between these two compartments. While almost all tissue cores are circAR3 positive, its levels vary between tumor cores. High Gleason tumors (Gleason score $\geq$ 8) have significant lower circAR3 expression than benign prostate (Figure 4C). The average circAR3 RISH score in low Gleason tumors (Gleason score $\leq$ 7) was in between benign

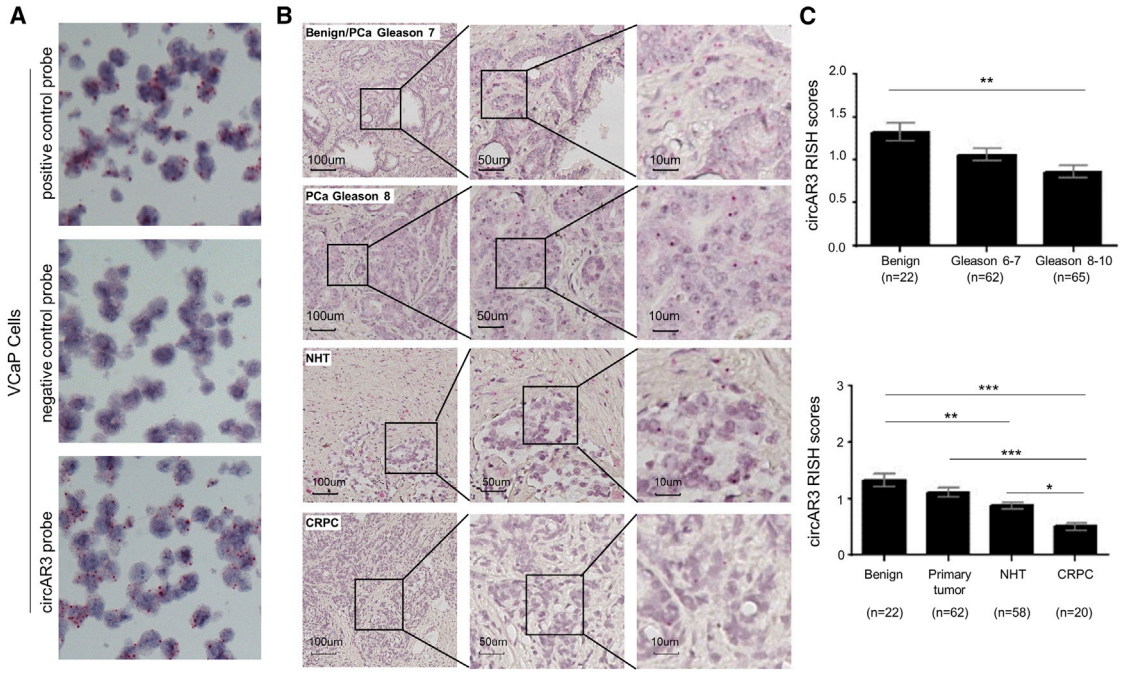

Figure 4. circAR3 Expression in PCa Tumor Samples

(A) VCaP cells were grown on glass coverslips and fixed using paraformaldehyde. RISH assays with control probes and the circAR3 probe were performed. (B) circAR3 RISH assays were performed on TMAs containing benign prostate, treatment-naive PCa, PCa treated with NHT, and CRPC tissue cores as reported.[39–42] Representative RISH images from each tumor group were presented. (C) RISH scores were evaluated as described in the Materials and Methods section. RISH scores were presented as the mean ± SD. Statistical analyses used one-way ANOVA test followed by Tukey's test with *p < 0.05, **p < 0.01, and ***p < 0.001.

prostate and high Gleason tumors. Compared to benign prostate and primary PCa, circAR3 expression was downregulated in tumors treated with neoadjuvant hormone therapy (NHT) and reached its lowest levels in CRPC cores. These results suggest that circAR3 expression is downregulated during tumor progression to CRPC.

Detection of circAR3 in PCa Patient Plasma

Since circAR3 can be secreted in conditioned media, it is likely detectable in serum from mouse bearing human PCa xenografts and PCa patient plasma. To test this hypothesis, we first established circAR3-positive LNCaP xenografts (n = 5) and circAR3-negative PC3 xenografts (n = 5) in nude mice. Mice were sacrificed when xenografts reached 1,000 mm^3 and total mouse serum was collected. All serum collected from mice with LNCaP tumors contained ~200–300 copies/mL of circAR3, while circAR3 was undetectable in mice with PC3 xenografts (Figure 5A). We showed that ~90% of circAR3, but not AR-fl, remained in the mouse serum even after it was kept at room temperature for up to 4 h (Figure 5B). Pearson's chi-square analysis showed that tumor volumes were highly correlated with serum circAR3 levels ($r = 0.88$, $p < 0.05$) (Figure 5C). These results indicated that tumor origin circAR3 can be detected in the serum of mice bearing circAR3 positive xenografts.

To determine whether circAR3 can be detected in PCa patient plasma, we initiated a pilot study by collecting plasma from 91 patients with benign prostate or primary PCa. Patient information, including Gleason scores, serum PSA levels at diagnosis, pathological stage, and lymph node metastasis status, is summarized (Table 1). We detected very low levels of plasma circAR3 in patients with benign prostate (Figure 5D). The majority of the plasma samples had undetectable levels of circAR3 with quantitative real-time PCR CT values below the detection threshold. circAR3 levels were elevated in PCa patients. Patients with high Gleason tumors have significantly higher circAR3 than patients with low Gleason tumors. Patients with lymph node metastasis had higher circAR3 than patients without lymph node metastasis (Figure 5E). However, circAR3 concentrations were not correlated with serum prostate specific antigen (PSA) levels (Figure 5F). To test whether plasma circAR3 originates from prostate or prostate tumors, we collected plasma from 10 patients before and after radical prostatectomy. All patient PSA levels dropped to < 0.1 ng/mL after surgery, indicating complete removal of the prostate tissue and cancer. All 10 patients who had circAR3 in their plasma before surgery became negative (below the detection threshold) after surgery (Figure 5G). These results support that plasma circAR3 is from prostate/PCa tissue.

circAR3 Does Not Affect AR Signaling, Cell Proliferation, and Invasion of PCa Cells

To determine whether circAR3 exerts any biological effect on PCa cells, we constructed plasmid vectors encoding circAR3 (Figure 6A).

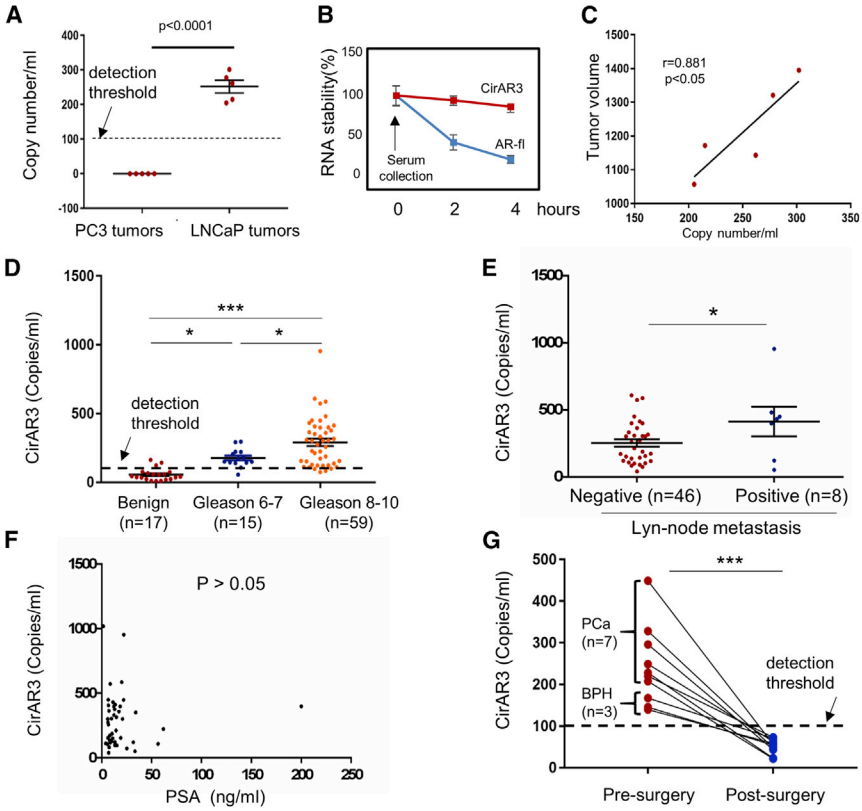

Figure 5. circAR3 Is Detectable in Serum of Xenograft-Bearing Mice and PCa Patients

(A) LNCaP and PC3 xenografts (n = 5) were established. Serum was collected when xenografts reached 1,000 mm^3. circAR3 copy numbers were determined by quantitative real-time PCR. Student's t test was used to compare circAR3 between the two tumor groups. (B) Serum collected from mice with LNCaP tumors was kept at room temperature for 0–4 h. Total RNA was extracted at either 0, 2, or 4 h. Relative circAR3 and AR-fl RNA levels were determined by quantitative real-time PCR and normalized from that of hour 0. (C) Correlation between circAR3 copy numbers with tumor volumes were calculated by Pearson's chi-square test. (D) Plasma was collected from 91 patients who had been diagnosed with either BPH or PCa as described in the Materials and Methods section. 1 mL of plasma from each patient sample was used for RNA extraction and quantitative real-time PCR. circAR3 copy numbers were determined by quantitative real-time PCR using absolute quantification. (E) Patients were grouped by lymph node metastasis status based on the pathology results after prostatectomy. Plasma circAR3 levels were compared between patient groups with −/+ lymph node metastasis. (F) Correlation of plasma circAR3 copy numbers with serum PSA levels was calculated by Pearson's chi-square test. (G) Three BPH and seven PCa patients had plasma collected both before and after prostatectomy. circAR3 copy numbers were determined by quantitative real-time PCR. Student's t test was used to compare circAR3 the differences pre- and post-surgery of the patients.

Three vectors were constructed, circAR3-LE (low expression), circAR3-HE (high expression), and circAR3-NC (negative control) as described in the Materials and Methods section. Authentication of circAR3 transcribed by these vectors was performed by RNase R treatment and small interfering RNA (siRNA) targeting the back-splice site (Figures 6B–6D). To determine whether circAR3 regulates AR transcriptional activities, LNCaP cells were transfected with the circAR3-HE vector. We found that mRNA levels of AR-regulated genes were not changed in the presence of −/+DHT. These genes include both androgen-dependent (e.g., NKX3.1 and TMPRSS2) and AR-independent (e.g., CDK1 and UBE2C) target genes. (Figure 6E). circAR3 did not alter AR protein expression and AR transcriptional activities (Figures 6F and 6G). circAR3 did not affect LNCaP cell proliferation and PC3 cell invasion (Figures 6H and 6I). These results indicate that AR signaling, PCa cell proliferation, and invasion were not regulated by circAR3.

DISCUSSION

To our knowledge, this is the first study to demonstrate that circAR3 is detectable in patient plasma in a prostate/PCa-specific manner. An optimized qPCR method was developed to measure circAR3 copy numbers with a sensitivity as low as 100 copies. We showed that plasma circAR3 levels are positively associated with Gleason scores and lymph node metastasis of primary tumors. These findings bring new insights into the potential of plasma circAR3 to be a biomarker to identify patients with higher risk PCa.

Our study showed that plasma circAR3 is derived from the prostate/PCa because they are undetectable after radical prostatectomy in patients with detectable levels prior to surgery. There are several ways for cell-free circAR3 to be released into the plasma from the prostate/PCa: (1) it can be passively released when cell death is induced by hypoxia, inflammation, or anti-cancer therapies, and (2) it can also be positively secreted in forms of exosomes into the bloodstream. Similar to PSA, release of circAR3 may also be affected by the integrity of prostate structures. The normal prostatic epithelium is isolated from prostate stroma by basal cells. Luminal epithelial cells are connected by tight junctions on the side and an apical surface-facing lumen for secretion. During PCa development, disappearance of basal cells and loss of tight junctions may promote circAR3 from epithelial cells to infiltrate into stoma and bypass endothelial cells into the bloodstream. In addition, hormonal and chemotherapies will also destruct stromal structure that may also contribute to circAR3 release to circulation system. Here, we report that circAR3 levels in tumors are negatively associated with tumor Gleason scores, while circAR3 levels in plasma are positively associated with high Gleason scores and positive lymph node metastasis. These findings suggest that there are increases of circAR3 to be released from prostate tumor cells into plasma during PCa

development and that circAR3 may be a possible marker for high-risk primary PCa.

Whether plasma circAR3 is an indicator of aberrant AR-v7 RNA splicing or *AR* gene overexpression and amplification of CRPC tumors needs further investigation. Plasma circAR3 concentrations may be determined by several rate-limiting factors: (1) circAR3 biosynthesis relies on the AR gene to be actively transcribed into AR pre-mRNA, a pre-requisite for circAR3, AR-fl, and AR-v7 to be synthesized. AR inhibition enhances the transcription rate of the AR gene, resulting in elevated circAR3, AR-fl, and AR-v7 levels in AR-positive PCa cells (Figure 3). (2) We observed that VCaP and 22Rv1 cells express higher levels of circAR3 than LNCaP cells, suggesting that more copies of exon3 in these cell lines may be correlated to relatively higher levels of intracellular circAR3. (3) RNA spliceosome may prioritize AR mRNAs to be synthesized over AR circRNAs under conditions of AR inhibition. We observed in PCa cell lines that alteration of circAR3 is not proportional to AR-fl and AR-v7 in the presence of AR antagonism (Figure 2), and these changes are in a cell-context-dependent manner (Figure 3). Considering the heterogeneity of PCa, each cancer cell within a tumor will respond to AR inhibition differently when synthesizing circAR3, AR-fl, and AR-v7. And (4), circAR3 may be more enriched in exosome and more resistant to RNA exonuclease degradation in plasma than linear AR mRNAs. Because of these rate-limited factors, it is difficult to postulate that plasma circAR3 is proportionally associated with *AR* gene splicing, overexpression, and amplification in CRPC that were frequently observed. Further investigation using matched PCa tissues and patient plasma samples before and post-CRPC progression from a larger patient cohort may provide insight on cirAR3 as a prognosis marker of CRPC in reflecting the *AR* gene alteration.

In summary, we report that circAR3 is widely expressed in prostate tumor cells. Prostate/PCa origin circAR3 is detectable in patient plasma. Increased expression of plasma circAR3 in patients with high Gleason tumors and lymph node metastasis suggest that circAR3 may be a biomarker of high-risk primary PCa.

MATERIALS AND METHODS

Tissue Culture

LNCaP, VCaP, PC3, 22Rv1, DU145, NCI-H660, and 293T cells were purchased from ATCC (Manassas, VA, USA). BPH cells were provided by Dr. Simon Hayward from the NorthShore University of HealthSystem. C4-2 cells were from Dr. Leland Cheung from Cedars Sinai. LNCaP95 cells are from Dr. Alan Meeker from John Hopkins University. Culture conditions were reported previously.[33–35]

RNA Extraction and RT-PCR

RNA was extracted by TRIzol-LS (Invitrogen) and purified by a Purelink RNA isolation kit (Ambion, Burlington, ON, Canada) according to the manufacture's instruction. The concentration and quality of extracted RNA was determined by NanoDrop (Thermo Scientific). For RT-PCR, RNA was treated with deoxyribonuclease and reverse transcribed. cDNA was used as a template to perform PCR, as we reported previously.[36]

Genomic DNA Isolation

Cells ($\sim 1 \times 10^5$) were lysed in 300 μL of DNA lysis buffer (100 mM Tris-HCL [pH 8.0], 5 mM EDTA [pH 8.0], 200 mM NaCl, 0.2% SDS, and 0.5 mg/mL Proteinase K) in 56°C for 16 h. After centrifugation at 12,000 rpm for 10 min, genomic DNA in the supernatant was precipitated with 750 μL of 100% ethanol and pelleted by centrifugation at 12,000 rpm for 10 min. The DNA pellet was dissolved in nuclease-free water.

Transient Transfection

Plasmid DNA and siRNA were transfected using lipofectamine3000 (Life Technologies) according to the manufacturer's instruction. Total RNA or protein was extracted 48 h after transfection for further analyses as we reported.[33–35] The sequence of siRNA targeting circAR3 back-splice site is 5′-gac tct ggg agg gaa aca gaa gt-3′ from Dharmacon.

Quantitative Real-Time PCR

Quantitative real-time PCR was performed on the ABI PRISM 7900 HT system (Applied Biosystems) with 5 ng of cDNA, 1 μM of each primer pair, and SYBR green PCR master mix (Roche, Laval, QC, Canada) following the manufacturer's instruction. All quantitative real-time PCR assays were carried out using three technical replicates and three independent cDNA syntheses. Primers used to amply circAR3 are 5′-gtc cat ctt gtc gtc ttc gga and 3′-caa tca ttt ctg ctg gcg ca. Primers used to measure AR-v7 and AR-fl were previously reported.[35,37] Relative quantification of quantitative real-time PCR data used glyceraldehyde 3-phosphate dehydrogenase (GAPDH) as the housekeeping gene.

For absolute quantification of quantitative real-time PCR, AR-fl and AR-v7 expression vectors and pSK-cARtemp were used as templates. Plasmid DNAs were quantified by NanoDrop (Thermo Scientific, Wilmington, DE, USA), and their copy numbers were calculated as follows: copy number (molecules/μL) = concentration (g/μL)/(bp size of double-stranded product × 660) × 6.022×10^{23}. A 10-fold serial dilution of each plasmid was made and used as a template to generate standard curves of log10 copy numbers versus the corresponding CT. The absolute quantity of circAR3, AR-fl, and AR-v7 in query samples were calculated by the standard curve according to their CT values.

Tissue Microarrays (TMAs) and RNA *In Situ* Hybridization (RISH)

Prostate tumor samples were retrieved from Vancouver Prostate Centre tissue bank under the approval of the Research Ethics Committee of the University of British Columbia (#H09-01628) and were used to build several TMAs that we previously reported.[34,38] The treatment-naive TMA contains 22 benign tissue cores, 62 primary PCas cores with Gleason scores of 6–7, and 65 primary PCas with Gleason scores of 8–10. The survival TMA contains 22 benign tissue cores, 62 primary PCa cores, 58 cores of PCa that received NHT, and 20 CRPC cores. CRPC samples were from patients who

Table 1. Patient Information Is Related to Figure 5

Parameter	Values
PSA at diagnosis (ng/mL)	18.91 ± 25.4
BPH patients	17
PCa patients	74
Gleason Group	
3 + 3	2
3 + 4	10
4 + 3	3
4 + 4	30
9 and 10	29
Clinical Stage	
T1c	27
T2a	14
T2b	11
T2c	2
T3c	7
unknown	13
Lymph Node Status	
Positive	8
Negative	46
unknown	20

had received hormonal therapies and been diagnosed with CRPC. The recurred tumors were removed by transurethral resection prostatectomy to relieve obstructive symptoms.

A specific RISH probe covering the back-splice site of circAR3 (cat. #715141), a positive control probe targeting human PPIB gene (cat. #710171), and a negative control probe targeting the dapB gene from bacteria (cat. #701021) were purchased from Advanced Cell Diagnostic (Hayward, CA, USA). RISH assays were performed using the BaseScope assay kit as we reported.[39–42] All stained slides were scanned by a Leica SCN400 scanner and digital images were evaluated by pathologist Dr. Ladan Fazli. RISH signal was presented as red dots or dot clusters and was evaluated under 40× magnification. circAR3 RISH signal was scored as zero if there was no RISH signal, one if RISH signal was positive in < 33% all cells within a core, two if RISH signal was positive in 33%–66% of the cells within a core, or three if RISH signal was positive in > 66% of the cells in a core.

Human Prostate Cancer Xenografts

LNCaP and PC3 cells (2×10^6 cells/per line) were implanted subcutaneously in bilateral flanks of 6- to 8-week-old male nude mice (n = 5). Tumor volume (V = length × width × height × 0.5236) was measured weekly. When tumor exceeded 1,000 mm^3, mice were sacrificed and mouse serum was collected immediately. All animal procedures were under the guidelines of the Canadian Council on Animal Care.

Patient Plasma Collection

We enrolled 91 patients who were diagnosed with benign prostatic hyperplasia or PCa by histology, PSA levels, and radiographic imaging from the Department of Urologic Sciences, Vancouver General Hospital, University of British Columbia (ethics certificate #H09-01628), the Department of Urology of the First Affiliated Hospital of Zhejiang University (ethics certificate #2018-819), and the Department of Urology at Zhejiang People's Hospital (ethics certificate #2019QT002) between April 2017 and February 2019. Patient information was shown in Table 1. There are 10 patients whose blood was collected twice, one before prostatectomy and one 6 weeks after surgery when PSA reduced to < 0.1 ng/mL. Whole blood was collected in Streck tubes and centrifuged at 1,600 × *g* for 15 min, after which plasma was transferred to a new tube and spun for another 1,600 × *g* for 10 min. Aliquots of cell-free plasma were stored at −80°C before RNA extraction. One-microliter plasma was used to perform RNA extraction and reverse transcription. To measure circAR3 copy numbers in patient plasma, the cDNA as well as serial diluted pSK-cARtemp were used as templates for the initial eight cycles of PCR using primers of F′ taa tac gac tca cta tag ggt gtc cat ctt gtc gtc ttc g and R′ att aac cct cac taa agg ga g gcg cac agg tac ttc tgt. It was followed by quantitative real-time PCR described above using primers 5′-taa tac gac tca cta tag gg-3′ and 5′-att aac cct cac taa agg ga-3′.

Construction of circAR3 Expression Vectors

Human genomic BAC clone (RP11-75E16) was retrieved from the Centre for Applied Genomics, the Hospital for Sick Children, University of Toronto. It was used as a template to amplify human androgen receptor exon 3 and its flanking regions by Platinum Taq DNA polymerase high fidelity (Invitrogen) and cloned into pCMV2-Flag vector (Sigma) as indicated (Figure 6A). Three vectors were made. The circAR3-LE vector contains AR exon 3, and 1,000 bp of 5′ intron sequences and 200 bp of 3′ intron sequences next to exon 3. The circAR3-HE vector was built on circAR3-LE with the 800 bp of 5′ intron sequences in reversed position inserted into 3′ splice site of exon 3. Lastly, the circAR3-NC has the same sequences to circAR3-HE, except exon 3 was deleted. All clones were confirmed by DNA Sanger sequencing.

Immunoblotting and Luciferase Reporter Assays

Immunoblotting assays were performed as we previously reported.[33–35] Cells were transfected with PSA-luciferase reporter plasmid with the renilla reporter as a control for transfection efficiency. Luciferase activities were determined using the luciferin reagent (Promega, Madison, WI, USA) according to the manufacturer's protocol. Transfection efficiency was normalized by renilla luciferase activity.

Cell Proliferation and Invasion Assays

Cell proliferation and invasion assays were previously described.[33–35] Cell proliferation assays were performed using the MTS (Promega) reagent according to the manufacturer's protocol. Cell proliferation rates were calculated as relative fold change of optical density 490 (OD_{490}). Cell invasion assays were carried out by using BD BioCoat

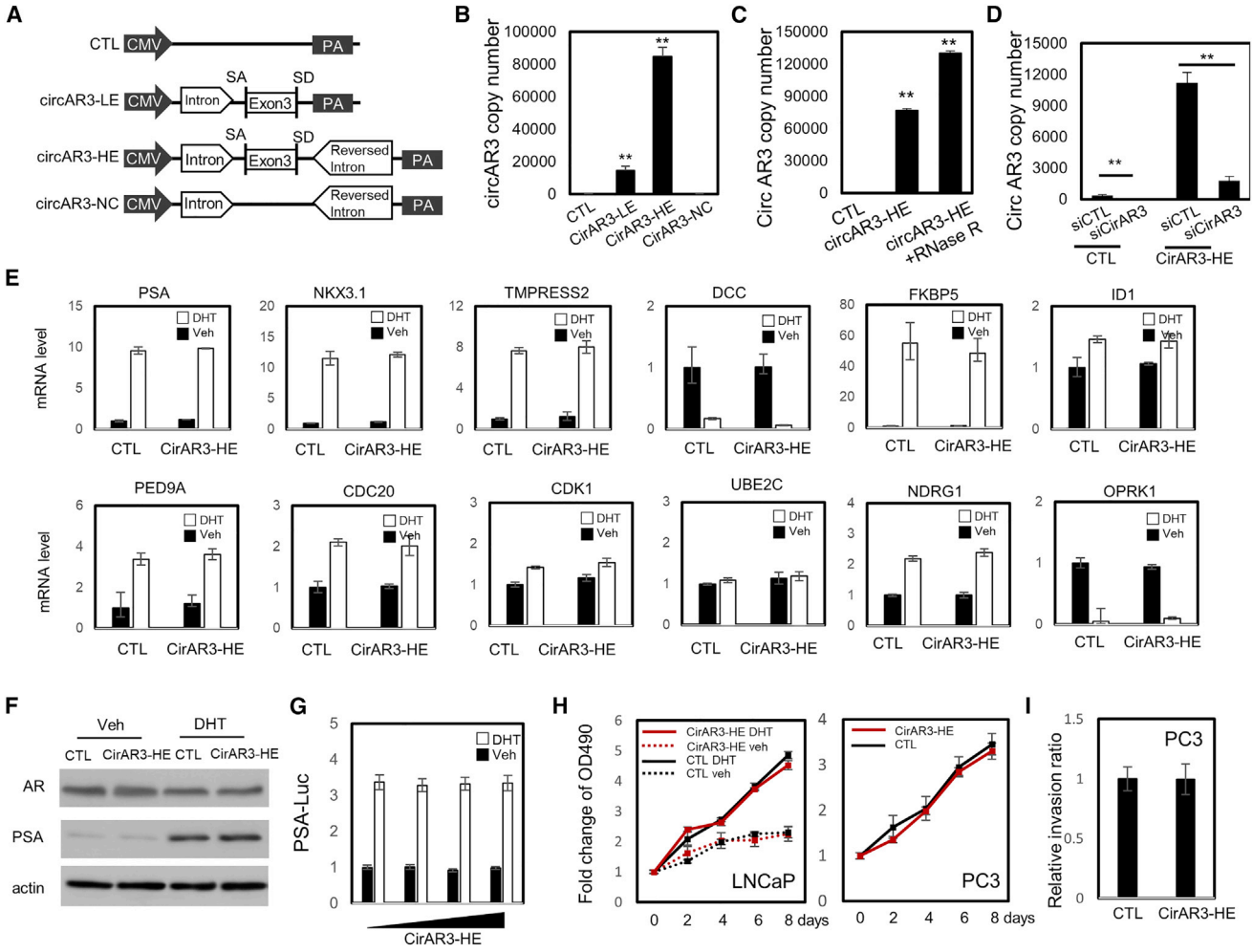

Figure 6. circAR3 Does Not Affect AR Signaling, Cell Proliferation, and Invasion of PCa Cells

(A) Schematic diagrams of expression vectors were constructed to express circAR3. The pCMV2 vector from Sigma was the control (CTL) vector. The construction of circAR3 vectors was as described in the Materials and Methods section. CMV, cytomegalovirus promoter; PA, polyadenylation signal; SA, splicing acceptor, SD, splicing donor. (B) AR-negative 293T cells were transfected with the designated plasmid vectors. circAR3 RNA levels were determined by quantitative real-time PCR using the absolute quantification method. (C) 293T cells were transfected with the circAR3-HE vector. After 24 h, RNA was extracted and treated with vehicle or RNase R for 1 h. circAR3 copy numbers were determined by quantitative real-time PCR using absolute quantification. (D) CTL or circAR3-HE vector was transfected into LNCaP cells. After 24 h, cells were transfected with either control siRNA or siRNA targeting circAR3. circAR3 mRNA levels were measured by quantitative real-time PCR using absolute quantification. (E) LNCaP cells were transfected with either control or circAR3-HE vector and treated with vehicle or 10 nM of DHT for 24 h. The mRNA expression of AR target genes was measured by quantitative real-time PCR assays. (F) AR and PSA protein expression was measured by immunoblotting with actin as a loading control. (G) LNCaP cells were transfected with increasing doses of circAR3-HE vector together with PSA-luciferase and renilla reporters. Cells were treated with vehicle or 10 nM of DHT for 24 h. Luciferase activities were measured as described in the Materials and Methods section. LNCaP (H) and PC3 (I) cells were transfected by control or circAR3-HE vector. LNCaP cells were also treated with vehicle or 10 nM of DHT. LNCaP cell proliferation rates and PC3 invasion rates were determined. All assays were repeated in three independent experiments that were performed in triplicate. One-way ANOVA followed by Tukey's test was used in pairwise comparison among different groups. Data were presented as the mean ± SD. **$p < 0.01$ when compared to controls.

Matrigel invasion chambers (BD Biosciences, USA) according to the manufacturer's protocol. Invasion rate was calculated as the percentage of cells invaded through the Matrigel.

Statistical Analysis

Statistical analysis was performed using the GraphPad Prism 6.0 software (GraphPad Software, CA, USA). One-way ANOVA followed by Tukey's test was used in pairwise comparison among different groups. circAR3 levels in correlation with PSA level and tumor volume were analyzed by Pearson's chi-square analysis. Student's t test was used to compare results between two experimental groups. The level of significance was set at *$p < 0.05$, **$p < 0.01$, and ***$p < 0.001$.

AUTHOR CONTRIBUTIONS

X.D. and M.G. conceived the study and designed the experiments. J.L., Y.L., W.Z., N.X., Y.S., Z.L., and L.F. performed experiments

and analyzed data. J.L., W.Z., D.Z., L.X., and M.G. provided human samples. X.D. wrote the manuscript.

ACKNOWLEDGMENTS

This work was supported by an operating grant from Zhejiang Provincial Natural Science Foundation of China (LY17H160019) to J.L.; a CIHR operating grant (MOP-137007) to X.D.; an industrial sponsored research grant from Three Cat Investments to X.D.; a Hunan Natural Sciences Foundation grant (2017JJ2370) to Z.L.; a visiting scholarship from Zhejiang Provincial People's Hospital to W.Z.; and visiting scholarships from China Scholar Council to Y.L. (201306231021) and Z.L. (201606375104).

REFERENCES

1. Scher, H.I., and Sawyers, C.L. (2005). Biology of progressive, castration-resistant prostate cancer: directed therapies targeting the androgen-receptor signaling axis. J. Clin. Oncol. *23*, 8253–8261.
2. Feldman, B.J., and Feldman, D. (2001). The development of androgen-independent prostate cancer. Nat. Rev. Cancer *1*, 34–45.
3. Scher, H.I., Fizazi, K., Saad, F., Taplin, M.E., Sternberg, C.N., Miller, K., de Wit, R., Mulders, P., Chi, K.N., Shore, N.D., et al.; AFFIRM Investigators (2012). Increased survival with enzalutamide in prostate cancer after chemotherapy. N. Engl. J. Med. *367*, 1187–1197.
4. de Bono, J.S., Logothetis, C.J., Molina, A., Fizazi, K., North, S., Chu, L., Chi, K.N., Jones, R.J., Goodman, O.B., Jr., Saad, F., et al.; COU-AA-301 Investigators (2011). Abiraterone and increased survival in metastatic prostate cancer. N. Engl. J. Med. *364*, 1995–2005.
5. Guo, Z., Yang, X., Sun, F., Jiang, R., Linn, D.E., Chen, H., Chen, H., Kong, X., Melamed, J., Tepper, C.G., et al. (2009). A novel androgen receptor splice variant is up-regulated during prostate cancer progression and promotes androgen depletion-resistant growth. Cancer Res. *69*, 2305–2313.
6. Hu, R., Dunn, T.A., Wei, S., Isharwal, S., Veltri, R.W., Humphreys, E., Han, M., Partin, A.W., Vessella, R.L., Isaacs, W.B., et al. (2009). Ligand-independent androgen receptor variants derived from splicing of cryptic exons signify hormone-refractory prostate cancer. Cancer Res. *69*, 16–22.
7. Li, Y., Chan, S.C., Brand, L.J., Hwang, T.H., Silverstein, K.A., and Dehm, S.M. (2013). Androgen receptor splice variants mediate enzalutamide resistance in castration-resistant prostate cancer cell lines. Cancer Res. *73*, 483–489.
8. Antonarakis, E.S., Lu, C., Wang, H., Luber, B., Nakazawa, M., Roeser, J.C., Chen, Y., Mohammad, T.A., Chen, Y., Fedor, H.L., et al. (2014). AR-V7 and resistance to enzalutamide and abiraterone in prostate cancer. N. Engl. J. Med. *371*, 1028–1038.
9. Sharp, A., Coleman, I., Yuan, W., Sprenger, C., Dolling, D., Rodrigues, D.N., Russo, J.W., Figueiredo, I., Bertan, C., Seed, G., et al. (2019). Androgen receptor splice variant-7 expression emerges with castration resistance in prostate cancer. J. Clin. Invest. *129*, 192–208.
10. Chen, C.D., Welsbie, D.S., Tran, C., Baek, S.H., Chen, R., Vessella, R., Rosenfeld, M.G., and Sawyers, C.L. (2004). Molecular determinants of resistance to antiandrogen therapy. Nat. Med. *10*, 33–39.
11. Robinson, D., Van Allen, E.M., Wu, Y.M., Schultz, N., Lonigro, R.J., Mosquera, J.M., Montgomery, B., Taplin, M.E., Pritchard, C.C., Attard, G., et al. (2015). Integrative clinical genomics of advanced prostate cancer. Cell *161*, 1215–1228.
12. Kumar, A., Coleman, I., Morrissey, C., Zhang, X., True, L.D., Gulati, R., Etzioni, R., Bolouri, H., Montgomery, B., White, T., et al. (2016). Substantial interindividual and limited intraindividual genomic diversity among tumors from men with metastatic prostate cancer. Nat. Med. *22*, 369–378.
13. Korpal, M., Korn, J.M., Gao, X., Rakiec, D.P., Ruddy, D.A., Doshi, S., Yuan, J., Kovats, S.G., Kim, S., Cooke, V.G., et al. (2013). An F876L mutation in androgen receptor confers genetic and phenotypic resistance to MDV3100 (enzalutamide). Cancer Discov. *3*, 1030–1043.
14. Joseph, J.D., Lu, N., Qian, J., Sensintaffar, J., Shao, G., Brigham, D., Moon, M., Maneval, E.C., Chen, I., Darimont, B., and Hager, J.H. (2013). A clinically relevant androgen receptor mutation confers resistance to second-generation antiandrogens enzalutamide and ARN-509. Cancer Discov. *3*, 1020–1029.
15. Conteduca, V., Wetterskog, D., Sharabiani, M.T.A., Grande, E., Fernandez-Perez, M.P., Jayaram, A., Salvi, S., Castellano, D., Romanel, A., Lolli, C., et al.; PREMIERE Collaborators; Spanish Oncology Genitourinary Group (2017). Androgen receptor gene status in plasma DNA associates with worse outcome on enzalutamide or abiraterone for castration-resistant prostate cancer: a multi-institution correlative biomarker study. Ann. Oncol. *28*, 1508–1516.
16. Armstrong, A.J., Halabi, S., Luo, J., Nanus, D.M., Giannakakou, P., Szmulewitz, R.Z., Danila, D.C., Healy, P., Anand, M., Rothwell, C.J., et al. (2019). Prospective Multicenter Validation of Androgen Receptor Splice Variant 7 and Hormone Therapy Resistance in High-Risk Castration-Resistant Prostate Cancer: The PROPHECY Study. J. Clin. Oncol. *37*, 1120–1129.
17. Tagawa, S.T., Antonarakis, E.S., Gjyrezi, A., Galletti, G., Kim, S., Worroll, D., Stewart, J., Zaher, A., Szatrowski, T.P., Ballman, K.V., et al. (2019). Expression of AR-V7 and ARv^{567es} in Circulating Tumor Cells Correlates with Outcomes to Taxane Therapy in Men with Metastatic Prostate Cancer Treated in TAXYNERGY. Clin. Cancer Res. *25*, 1880–1888.
18. Welti, J., Rodrigues, D.N., Sharp, A., Sun, S., Lorente, D., Riisnaes, R., Figueiredo, I., Zafeiriou, Z., Rescigno, P., de Bono, J.S., and Plymate, S.R. (2016). Analytical Validation and Clinical Qualification of a New Immunohistochemical Assay for Androgen Receptor Splice Variant-7 Protein Expression in Metastatic Castration-resistant Prostate Cancer. Eur. Urol. *70*, 599–608.
19. Scher, H.I., Lu, D., Schreiber, N.A., Louw, J., Graf, R.P., Vargas, H.A., Johnson, A., Jendrisak, A., Bambury, R., Danila, D., et al. (2016). Association of AR-V7 on Circulating Tumor Cells as a Treatment-Specific Biomarker With Outcomes and Survival in Castration-Resistant Prostate Cancer. JAMA Oncol. *2*, 1441–1449.
20. Miyamoto, D.T., Lee, R.J., Stott, S.L., Ting, D.T., Wittner, B.S., Ulman, M., Smas, M.E., Lord, J.B., Brannigan, B.W., Trautwein, J., et al. (2012). Androgen receptor signaling in circulating tumor cells as a marker of hormonally responsive prostate cancer. Cancer Discov. *2*, 995–1003.
21. Azad, A.A., Volik, S.V., Wyatt, A.W., Haegert, A., Le Bihan, S., Bell, R.H., Anderson, S.A., McConeghy, B., Shukin, R., Bazov, J., et al. (2015). Androgen Receptor Gene Aberrations in Circulating Cell-Free DNA: Biomarkers of Therapeutic Resistance in Castration-Resistant Prostate Cancer. Clin. Cancer Res. *21*, 2315–2324.
22. Markowski, M.C., Silberstein, J.L., Eshleman, J.R., Eisenberger, M.A., Luo, J., and Antonarakis, E.S. (2017). Clinical Utility of CLIA-Grade AR-V7 Testing in Patients With Metastatic Castration-Resistant Prostate Cancer. JCO Precis. Oncol. 2017. https://doi.org/10.1200/PO.17.00127.
23. Pasut, A., Matsumoto, A., Clohessy, J.G., and Pandolfi, P.P. (2016). The pleiotropic role of non-coding genes in development and cancer. Curr. Opin. Cell Biol. *43*, 104–113.
24. Bach, D.H., Lee, S.K., and Sood, A.K. (2019). Circular RNAs in Cancer. Mol. Ther. Nucleic Acids *16*, 118–129.
25. Guo, J.U., Agarwal, V., Guo, H., and Bartel, D.P. (2014). Expanded identification and characterization of mammalian circular RNAs. Genome Biol. *15*, 409.
26. Salzman, J., Gawad, C., Wang, P.L., Lacayo, N., and Brown, P.O. (2012). Circular RNAs are the predominant transcript isoform from hundreds of human genes in diverse cell types. PLoS ONE *7*, e30733.
27. Vo, J.N., Cieslik, M., Zhang, Y., Shukla, S., Xiao, L., Zhang, Y., Wu, Y.M., Dhanasekaran, S.M., Engelke, C.G., Cao, X., et al. (2019). The Landscape of Circular RNA in Cancer. Cell *176*, 869–881.e13.
28. Chen, S., Huang, V., Xu, X., Livingstone, J., Soares, F., Jeon, J., Zeng, Y., Hua, J.T., Petricca, J., Guo, H., et al. (2019). Widespread and Functional RNA Circularization in Localized Prostate Cancer. Cell *176*, 831–843.e22.
29. Ashwal-Fluss, R., Meyer, M., Pamudurti, N.R., Ivanov, A., Bartok, O., Hanan, M., Evantal, N., Memczak, S., Rajewsky, N., and Kadener, S. (2014). circRNA biogenesis competes with pre-mRNA splicing. Mol. Cell *56*, 55–66.

30. Jeck, W.R., Sorrentino, J.A., Wang, K., Slevin, M.K., Burd, C.E., Liu, J., Marzluff, W.F., and Sharpless, N.E. (2013). Circular RNAs are abundant, conserved, and associated with ALU repeats. RNA *19*, 141–157.

31. Li, Y., Zheng, Q., Bao, C., Li, S., Guo, W., Zhao, J., Chen, D., Gu, J., He, X., and Huang, S. (2015). Circular RNA is enriched and stable in exosomes: a promising biomarker for cancer diagnosis. Cell Res. *25*, 981–984.

32. Kuruma, H., Matsumoto, H., Shiota, M., Bishop, J., Lamoureux, F., Thomas, C., Briere, D., Los, G., Gleave, M., Fanjul, A., and Zoubeidi, A. (2013). A novel antiandrogen, Compound 30, suppresses castration-resistant and MDV3100-resistant prostate cancer growth in vitro and in vivo. Mol. Cancer Ther. *12*, 567–576.

33. Li, Y., Donmez, N., Sahinalp, C., Xie, N., Wang, Y., Xue, H., Mo, F., Beltran, H., Gleave, M., Wang, Y., et al. (2017). SRRM4 Drives Neuroendocrine Transdifferentiation of Prostate Adenocarcinoma Under Androgen Receptor Pathway Inhibition. Eur. Urol. *71*, 68–78.

34. Li, H., Xie, N., Chen, R., Verreault, M., Fazli, L., Gleave, M.E., Barbier, O., and Dong, X. (2016). UGT2B17 Expedites Progression of Castration-Resistant Prostate Cancers by Promoting Ligand-Independent AR Signaling. Cancer Res. *76*, 6701–6711.

35. Liu, L.L., Xie, N., Sun, S., Plymate, S., Mostaghel, E., and Dong, X. (2014). Mechanisms of the androgen receptor splicing in prostate cancer cells. Oncogene *33*, 3140–3150.

36. Liu, L., Xie, N., Rennie, P., Challis, J.R., Gleave, M., Lye, S.J., and Dong, X. (2011). Consensus PP1 binding motifs regulate transcriptional corepression and alternative RNA splicing activities of the steroid receptor coregulators, p54nrb and PSF. Mol. Endocrinol. *25*, 1197–1210.

37. Li, Y., Xie, N., Gleave, M.E., Rennie, P.S., and Dong, X. (2015). AR-v7 protein expression is regulated by protein kinase and phosphatase. Oncotarget *6*, 33743–33754.

38. Yu, Y., Yang, O., Fazli, L., Rennie, P.S., Gleave, M.E., and Dong, X. (2015). Progesterone receptor expression during prostate cancer progression suggests a role of this receptor in stromal cell differentiation. Prostate *75*, 1043–1050.

39. Li, Y., Zhang, Q., Lovnicki, J., Chen, R., Fazli, L., Wang, Y., Gleave, M., Huang, J., and Dong, X. (2019). SRRM4 gene expression correlates with neuroendocrine prostate cancer. Prostate *79*, 96–104.

40. Gan, Y., Li, Y., Long, Z., Lee, A.R., Xie, N., Lovnicki, J.M., Tang, Y., Chen, X., Huang, J., and Dong, X. (2018). Roles of Alternative RNA Splicing of the Bif-1 Gene by SRRM4 During the Development of Treatment-induced Neuroendocrine Prostate Cancer. EBioMedicine *31*, 267–275.

41. Lee, A.R., Gan, Y., Xie, N., Ramnarine, V.R., Lovnicki, J.M., and Dong, X. (2019). Alternative RNA splicing of the GIT1 gene is associated with neuroendocrine prostate cancer. Cancer Sci. *110*, 245–255.

42. Long, Z., Li, Y., Gan, Y., Zhao, D., Wang, G., Xie, N., Lovnicki, J.M., Fazli, L., Cao, Q., Chen, K., and Dong, X. (2019). Roles of the HOXA10 gene during castrate-resistant prostate cancer progression. Endocr. Relat. Cancer *26*, 279–292.